HHS Public Access

Author manuscript

Endocr Relat Cancer. Author manuscript; available in PMC 2020 October 01.

Published in final edited form as:

Endocr Relat Cancer. 2019 October ; 26(10): 765–778. doi:10.1530/ERC-19-0262.

Targeting PDZ Binding Kinase Is Anti-tumorigenic in Novel Preclinical Models of ACC

Adwitiya Kar[1], **Yu Zhang**[1], **Betelehem W. Yacob**[2], **Jordan Saeed**[1], **Kenneth D. Tompkins**[1], **Stacey M. Bagby**[2], **Todd M. Pitts**[2], **Hilary Somerset**[3], **Stephen Leong**[2], **Margaret E. Wierman**[1,4], **Katja Kiseljak-Vassiliades**[1,4]

[1]Division of Endocrinology, Metabolism and Diabetes, Department of Medicine, University of Colorado School of Medicine Anschutz Medical Campus Aurora, CO 80045

[2]Division of Medical Oncology, Department of Medicine, University of Colorado School of Medicine Anschutz Medical Campus Aurora, CO 80045

[3]Department of Pathology, University of Colorado School of Medicine Anschutz Medical Campus Aurora, CO 80045

[4]Research Service, Rocky Mountain Regional Veterans Affairs Medical Center, Aurora, CO 80045

Abstract

Adrenocortical carcinoma (ACC) is an aggressive orphan malignancy with less than 35% 5-year survival and 75% recurrence. Surgery remains the primary therapy and Mitotane, an adrenolytic, is the only FDA approved drug with wide range toxicities and poor tolerability. There are no targeted agents available to date. For the last three decades, H295R cell line and its xenograft were the only available pre-clinical models. We recently developed two new ACC patient derived xenograft mouse models and corresponding cell lines (CU-ACC1 and CU-ACC2) to advance research in the field. Here, we have utilized these novel models along with H295R cells to establish the mitotic PDZ binding kinase (PBK) as a promising therapeutic target. *PBK* is overexpressed in ACC samples and correlates with poor survival. We show that PBK is regulated by FOXM1 and targeting PBK via shRNA decreased cell proliferation, clonogenicity, and anchorage independent growth in ACC cell lines. PBK silencing inhibited pAkt, pp38MAPK, and pH3 altering the cell cycle. Therapeutically, targeting PBK with the small molecule inhibitor HITOPK032 phenocopied PBK specific modulation of pAkt and pH3, but also induced apoptosis via activation of JNK. Consistent with *in vitro* findings, treatment of CU-ACC1 PDXs with HITOPK032 significantly reduced tumor growth by 5-fold ($p < 0.01$). Treated tumor tissues demonstrated increased rates of

Corresponding author and person to whom reprints requests should be addressed: Katja Kiseljak-Vassiliades, DO, Endocrinology MS8106, University of Colorado School of Medicine, 12801 East 17th Ave, RC1 South, Aurora, CO 80045, USA, Phone: 303-724-3951, Fax: 303-724-3920. katja.kiseljak-vassiliades@ucdenver.edu.

Author Contribution statement

Conception and design: A. Kar, K. Kiseljak-Vassiliades, M. E. Wierman

Development of methodology: A. Kar, Y. Zhang

Acquisition of data: A. Kar, Y. Zhang, J. Saeed, S. Bagby, B. Yacob

Analysis and interpretation of data: A. Kar, K. Kiseljak-Vassiliades

Writing, review, and/or revision of manuscript: A. Kar, K. Kiseljak-Vassiliades, M.E. Wierman

Administrative, technical, or material support: T. Pitts, S. Leong, K. Kiseljak-Vassiliades, H. Somerset, M.E. Wierman

Study supervision: K. Kiseljak-Vassiliades, M.E. Wierman

Declaration of interest: The authors declare no potential conflicts of interest

apoptosis and JNK activation, with decreased pAkt and H3 phosphorylation, consistent with effects observed in ACC cell lines. Together these studies elucidate the mechanism of PBK in ACC tumorigenesis and establish the potential therapeutic potential of HITOPK032 in ACC patients.

Keywords

Adrenocortical carcinoma; PBK; MAPK; Apoptosis; PDX

Introduction

Adrenocortical carcinoma (ACC) is an aggressive rare cancer affecting 1–2 person per-million-per-year with a 5-year survival less than 35% (Else, et al. 2014; Mohan, et al. 2018). Surgery is the first line treatment for localized disease, but therapeutic options are limited for metastatic disease or recurrence (Mohan et al. 2018). Mitotane, an adrenolytic agent, is the only FDA approved drug with modest benefits (Hahner and Fassnacht 2005; Libe 2015; Mohan et al. 2018). Systemic chemotherapy with EDP (etoposide, doxorubicin, and cisplatin) is associated with a 5-month progression free survival (Mohan et al. 2018). The limited effectiveness of currently used approaches underscores the need for new therapies for patients with ACC (Berruti, et al. 2017; Mohan et al. 2018). Integrated genomic studies have revealed that 60% of ACC tissues harbor frequent mutations in *TP53, ATM, CTNNB1*, none of which have been successfully targeted up to date (Else et al. 2014). In addition, 40% of ACC tumors have no known drivers (Assie, et al. 2014; Zheng, et al. 2016). *IGF2* overexpression has long been considered an important molecular marker of ACC; however, targeting of the IGFR1 receptor yielded disappointing results in clinical trials (Barlaskar, et al. 2009; Beuschlein, et al. 2016; Boulle, et al. 2001; Fassnacht, et al. 2015). Previous attempts to target VEGF and EGFR (Chau, et al. 2012; Quinkler, et al. 2008; Terzolo, et al. 2014) have also met with modest success, emphasizing the need for identification and characterization of novel targets in ACC.

Research in the ACC field has been stifled by the lack of pre-clinical models. In the last three decades, most *in vitro* and *in vivo* ACC research has been conducted using a single cell line and its derivative H295R (Wang and Rainey 2012). We recently developed two new patient derived xenografts (PDX) ACC and derived cell lines to advance research in this field (Kiseljak-Vassiliades, et al. 2018a). Using multiple gene expression microarray data sets comparing ACC, adrenal adenomas and normal adrenal (Kiseljak-Vassiliades, et al. 2018b), and consistent with published literature, we observed a dysregulation of cell cycle control genes and its pathway constituents (Kiseljak-Vassiliades et al. 2018b; Mohan et al. 2018). Most prominent was the upregulation of PBK, which has been established as master mitotic kinase known for its role in mitotic division and regulation (Abe, et al. 2007; Rizkallah, et al. 2015). PBK has been shown to have a critical role in cytokinesis (Abe et al. 2007; Matsumoto, et al. 2004; Matsuo, et al. 2014; Park, et al. 2010; Stauffer, et al. 2017) and in cellular proliferation via interaction with p53, modulation of p38MAPK and the DNA damage response (Hu, et al. 2010; Lei, et al. 2013; Nandi, et al. 2007). While PBK is not detectable in most normal human tissues, it is upregulated in several human cancers (Brown-

Clay, et al. 2015; Chang, et al. 2016; Dou, et al. 2015; He, et al. 2010), where it contributes to a more aggressive phenotype (Brown-Clay et al. 2015; Ohashi, et al. 2017; Park, et al. 2006). Targeting PBK with the small molecule inhibitors has been shown to reduce tumor growth or lead to tumor regression in xenograft cancer models (Joel, et al. 2015; Kim, et al. 2012; Matsuo et al. 2014; Wang, et al. 2016).

PBK is 12-fold increased in ACC tissues compared to normal adrenal samples. In H295R and the recently characterized CU-ACC1 and CU-ACC2 cells, PBK expression was associated with increased tumorigenesis and proliferation. Treatment with the PBK inhibitor, HITOPK032, blocked proliferation and triggered apoptosis in ACC cells, and decreased tumor growth in our newly established *in vivo* ACC PDX mouse model. Together these findings establish the importance of PBK as a pro-tumorigenic kinase in ACC and confirm its potential as a therapeutic target for our patients.

Materials and Methods

Analysis of public genomic data sets

Publically available microarray datasets containing normal adrenal (n= 14), adrenal adenoma (n=22) and ACC (n=77) gene expression were analyzed as previously described (Kiseljak-Vassiliades et al. 2018b). Data was analyzed using Partek Genomics Suite 6.6 with the false discovery rate of <0.05. With the focus on detecting druggable therapeutic targets, data was screened for differentially regulated kinase transcripts with > 2 fold differential expression between ACC and normal adrenal samples. Kaplan-Meier, clinical correlation between gene expression and survival outcomes were generated using Graph Pad with the TCGA dataset from cBioPortal for Cancer Genomics. RNA expression was normalized using RSEM. Samples with expression Z scores > 2 were considered dysregulated (Cerami, et al. 2012; Gao, et al. 2013).

Cell culture

H295R cells were grown in DMEM/F12 (50:50) media supplemented with 5% NuSerum, 1% Antibiotic Pen/Step. CU-ACC1 and CU-ACC2 cells were derived from their respective PDXs and grown in 3:1 (v/v) F-12/DMEM containing 10% fetal bovine serum and growth factors as previously described (Kiseljak-Vassiliades et al. 2018a; Kiseljak-Vassiliades et al. 2018b). All cells were grown at 37°C in a 5% CO_2 chamber.

Antibodies and reagents

The following primary antibodies were used for immunoblot analysis: PARP (#9542S), pH3 (Ser10) (#9701S), H3 (# 4499S), pAkt (Ser473) (#9271), Akt (#9272), pERK (p42/44) (9101S), ERK (#9102), pp38MAPK (#9211), p38MAPK (# 9212), pJNK (#9251S), JNK (# 9252) from Cell Signaling (Danvers, MA); FOXM1 (# SC-500) from Santa Cruz; β tubulin (#ab6046), PBK (# ab75983) from Abcam. For IHC anti-PBK (#4942S) was purchased from Cell Signaling. The FOXM1 inhibitor, thiostrepton, was obtained from EMD Millipore (Burlington, MA). PBK inhibitor HITOPK032 was purchased from Sigma (St Louis, MO).

Plasmids and transduction

Transfer plasmids were purchased from GE Dharmacon (Lafayette, CO) as part of the TRIPZ shRNA starter packaging kit (RHS5087). TRIPZ lentiviral doxycycline-inducible shPBK and shScr plasmids with a TurboRFP fluorescent reporter was bought from Dharmacon (RHS4740) and plasmids were packaged using packaging plasmid mix and transfection reagent in HEK293FT cells using the manufacture's protocol. Cells were transduced at a ratio of 1:3 of viral supernatant to media and were selected with 2ug/ml puromycin for CU-ACC1 and 10ug/ml for H295R to create stable lines. Doxycycline 2ug/ml was added to induce shPBK gene expression after stable selection. Cells were sorted for a high RFP signal.

Immunoblot Analysis

Samples were harvested in RIPA buffer, protein was quantified using BCA. Proteins were blotted on PVDF membrane and blocked using 3% BSA. For most proteins, membranes were incubated overnight with primary antibodies at 1:1000 dilution. Membranes were incubated with p-H3 and p-JNK antibody at 1:500 for two days before addition of the secondary antibody. HRP conjugated rabbit or mouse polyclonal IgG were used as secondary antibodies. Blots were developed using the Thermo Fisher Scientific ECL kit (Waltham, MA). Densitometry analysis was performed using the NIH Image J software. Figures are representative of at least three biological replicates.

Immunohistochemistry

Immunohistochemistry (IHC) for PBK and pH3 was performed on 5 micrometer thin sections prepared from formalin-fixed paraffin-embedded human ACC tumor samples and normal adrenal tissue. Sections were deparaffinized, hydrated, antigen retrieved with standard methods. Incubation with anti-PBK or anti-pH3 was done at 1:50 dilution overnight. Biotinylated anti-rabbit was used as secondary. Slides were developed using ABC elite Vectastain kit (Vector lab, Burlingame, CA) and DAB staining. Counterstaining was performed with Harris hematoxylin for one minute. Thereafter, slides were dehydrated following standard protocols and mounted with permount.

Quantitative Real-Time PCR

RNA was extracted using RNeasy kit (Qiagen) and reverse transcribed to cDNA (Iscript cDNA synthesis kit (Biorad). The Power SYBR green QPCR master mix from Life technologies was used for real-time quantitative analysis (Kiseljak-Vassiliades et al. 2018b).

Proliferation, clonogenicity, and soft agar assays

Proliferation assays were performed using the Incucyte ZOOM imaging system from Essen Biosciences (Ann Arbor, MI). Cells were plated at a concentration of 5000 cells/well in a 96-well plate. Standard scans were conducted under 4X magnification and images were quantified using Image J. Clonogenicity and soft assays were carried for 14 days and 21 days respectively, following protocols previously published (Kiseljak-Vassiliades et al. 2018b). Soft agar colonies were stained with Nitroblue tetrazolium salt and colonies were

counted from photographed images using an in built macro in Im age J software (Kar and Gutierrez-Hartmann 2017).

Double thymidine block and flow cytometry

ACC cell lines at 50% confluency were subjected to 2mM thymidine treatment for 15 hours followed by 9 hour release followed by an additional 18 hours of 2mM thymidine treatment. Cells were washed and released in normal media, and cells were either harvested for western blots in lysis buffer or stained with propidium iodide for flow cytometry analysis. Flow cytometry was performed at CU Cancer Center shared resources and histograms fitted using Modfit.

Caspase 3/7 assays

Cells were plated in 96-well in quadruplicates and treated with either HITOPK032 (2uM) (Sigma) or HITOPK032 in combination with SP600125 (10uM) (Selleckchem), a JNK inhibitor. Plates were incubated for 10 minutes and luminescence was measured using Promega's protocol for Caspase 3/7 glo assay with microplate reader.

Patient derived xenograft models

Female athymic nude mice were purchased form Harlan labs, and PDXs were generated as previously described (Kiseljak-Vassiliades et al. 2018a). Tumors were propagated bilaterally into 26 mice to obtain 7–9 evaluable tumors per group. When tumors reached 100–400 mm^3 mice were randomized into control and HITOPK032 treated groups. Mice received HITOPK032 10mg/kg daily by oral gavage for 17 days and were visually monitored for signs of toxicity. Tumors were measured twice a week by caliper and measurements were recorded in the Study Director Program (San Fran, CA). Volume was calculated using the formula (length x $width^2$) x 0.52. All studies were conducted under animal protocols approved by the University of Colorado Denver Institutional Animal Care and Use Committee.

Statistical Analysis

Data are presented as means ± SEM from three or more separate experiments. Densitometry analysis performed on immunoblots represent at least 3 biological replicates. P-values were calculated using unpaired Student's t-Test for two-group comparison or ANOVA (with Bonferroni posttest analysis for multiple comparisons). All data were analyzed and presented using GraphPad Prism software (version 5.0; GraphPad Software Inc., La Jolla, CA).

Results

PBK is upregulated in ACC and is correlated with poor survival outcomes in ACC patients

PBK transcript expression was 12-fold upregulated in ACC (n=77) compared to normal adrenals (n=14) ($p < 0.001$) and 7-fold higher compared to adrenal adenomas (n= 22) ($p < 0.001$) (Fig. 1A) in the analysis of publicly available microarray gene expression datasets (Kiseljak-Vassiliades et al. 2018b) . *PBK* expression was highly correlated with MK67(Ki

67) (Supplementary Fig.1), a major prognostic marker in ACC. Kaplan-Meier estimate of overall survival (OS) in the 75 cases available through cBioPortal (Gao et al. 2013) revealed that high *PBK* expression in the tumor was associated with significantly poorer overall survival (OS) ($p < 0.001$) with a median OS of 16.1 months (Fig. 1B), and a poorer disease free survival (DFS) ($p < 0.001$) with a median DFS of 5.31 months in patients with higher PBK transcript levels (Fig. 1C).

Immunoblotting of ACC samples (N=8, Fig. 1D) along with H295R, CU-ACC1, CU-ACC2 cell lines and respective PDXs (Fig. 1E) showed high PBK expression in ACC tissues, in H295R and CU-ACC1 cell lines, and in the CU-ACC1 and CU-ACC2 PDX. CU-ACC2 cells had 2.5 and 4 fold less PBK expression than H295R and CU-ACC1 cells, respectively. (Fig 1E, quantitative graph on right).

Examination of PBK subcellular localization (Fig. 1F) via immunohistochemistry exhibited only low levels of diffuse cytoplasmic PBK staining in normal adrenals, but strong nuclear as well as diffuse cytoplasmic staining in ACC tissues indicating that the nuclear location and higher PBK expression was strictly associated with adrenal carcinogenesis. Together these results further supported the potential oncogenic significance of PBK in ACC.

FOXM1 controls PBK expression in ACC cells

Prior work has established that FOXM1 regulates several mitotic kinases including MELK (maternal embryonic leucine zipper kinase) and PBK (Kato, et al. 2016). Silencing or targeting MELK or PBK in renal cancer cells decreased FOXM1 expression indicating a feedback loop (Kato et al. 2016). In our analysis, the TCGA ACC dataset (n=75) demonstrates a strong *PBK*-*FOXM1* co-expression with a Spearman $r_s = 0.903$ ($p < 0.001$) (Supplementary Fig. 2A). To examine whether FOXM1 controls PBK expression, H295R, CU-ACC1, and CU-ACC2 cells were treated with the FOXM1 inhibitor, thiostrepton, at doses of 0.5uM, 1uM, 3uM, and 5uM. *FOXM1* and *PBK* mRNA levels were assessed at 24 hours by qPCR (Supplementary Fig. 2B-D). Increasing doses of thiostrepton resulted in a ~1.6–10 fold dose dependent decrease of *FOXM1* expression followed by 2–10 fold decrease in *PBK* expression ($p < 0.05$–0.01). Immunoblotting showed a similar dose dependent decrease in PBK protein expression with thiostrepton treatment (Supplementary Fig. 2E-G), suggesting that FOXM1 is an upstream modulator of PBK in ACC. In contrast to studies in renal carcinoma (Kato et al. 2016), PBK silencing did not decrease FOXM1 protein expression (Supplementary Fig. 2H), suggesting that PBK does not regulate FOXM1 expression in a feedback loop in adrenal cancer.

Silencing PBK inhibits *in vitro* tumorigenesis in ACC and modulates Akt and MAPK signaling

Next, the functional role of PBK was examined using two different doxycycline-inducible lentiviral shRNAs (shPBK1 and shPBK3) and a scramble (shScr) control in *in vitro* models of CU-ACC1, H295R, and CU-ACC2 cells. Silencing with either construct was nearly complete in CU-ACC1 cell lines (Fig. 2A insert). In H295R and CU-ACC2 cells , 80% and 30% silencing was achieved with shPBK1 and shPBK3, respectively (Fig. 2D insert, Supplementary Fig. 3B). Incucyte live cell imaging assay (Fig. 2A) demonstrated that, by

day 10, there was on average a 6-fold decrease in proliferation with shPBK1 and shPBK3 in CU-ACC1 cells ($p<0.01$) , whereas a 2.6-fold decrease with shPBK1 and 1.9-fold decrease with shPBK3 ($p <0.01$) was observed in H295R cell lines compared to controls (Fig. 2D). There was also on average 2.2-fold decrease ($p < 0.01$) in 2D colony numbers with shPBK1 and shPBK3 in CU-ACC1 cells (Fig. 2B) and an average 6.6-fold decrease ($p <0.01$) in H295R cells (Fig. 2E). In both cell lines, inhibitory response correlated with the level of PBK silencing achieved. PBK silencing with either constructs also inhibited anchorage independent growth by 20 fold in CU-ACC1 cells (Fig. 2C $p<0.01$) and a 4.5-fold decrease with shPBK1 ($P <0.01$) and a 2.6-fold decrease in colony formation with shPBK3 ($p<0.01$) in H295R cells (Fig. 2F).

The CU-ACC2 cell line, which compared to CU-ACC2 PDX has lower expression of PBK, appeared most resilient to PBK knockdown, and showed no significant change in proliferative rates with PBK silencing (Supplementary Fig. 3A). Clonogenicity assays, considered more stringent than proliferative assays, showed a 3.7-fold decrease in colony numbers with shPBK1 ($p< 0.01$) and a 1.7-fold decrease with shPBK3 ($p<0.05$) (Supplementary Fig. 3B). Anchorage independent growth could not be assessed in this model as CU-ACC2 cells failed to form colonies in soft agar.

Since PBK has been implicated in modulation of PI3K and MAPK downstream pathways in other cancers (Ayllon and O'Connor 2007; Shinde, et al. 2013), we next assessed the activation of downstream effectors including pAkt (S473), p38MAPK (Thr180/Tyr182), and pERK (p42/44) in ACC cell lines. PBK silencing resulted on average in a 2-fold decrease in pAkt and 1.8–3 fold decrease in p38MAPK ($p<0.05$) with no effects on ERK activation (Fig. 2G, Supplementary Fig. 3C). Overall, the attenuation in the phosphorylation status correlated with the level of PBK silencing, underscoring PBK specific effects on downstream signaling in ACC cells.

PBK silencing alters cell cycle progression in CU-ACC1 cell line

In triple negative breast cancer, PBK has been shown to directly phosphorylate histone 3 (pH3), consistent with its role as a mitotic kinase (Park et al. 2006). We found that in non-synchronized cells, silencing PBK decreased pH3 on average by 5-fold in CU-ACC1 ($p <0.01$), 2-fold in H295R cells ($p <0.05$), and 1.5 fold in CU-ACC2 cell lines (Figure 3A, Supplementary Fig. 3C). Upon confirming that ACC cell lines can be synchronized at G1/S using a double thymidine treatment (Supplementary Fig. 4A), we assessed the effects of PBK silencing on histone 3 phosphorylation during cell cycle progression. Examination of pH3 through mitotic progression post block release showed that PBK knockdown completely inhibited induction of pH3 in synchronized CU-ACC1 cell (Supplementary Fig. 4B). The decrease was less prominent in PBK silenced H295R cells (Supplementary Fig. 4C), which based on pH3 induction also appeared to maintain the same timeline of mitotic entry and exit as the control cells. Flow cytometry was performed to specifically analyze if PBK silencing affects cell cycle progression in CU-ACC1 cells. Thymidine-blocked scramble control cells showed a 59% increase in S phase cells over asynchronous cells (Fig. 3B) further confirming effective synchronization at S phase. Next, percent of cells at different phases of cell cycle was examined in synchronized control and PBK silenced cells

via flow cytometry. Since CU-ACC1 cells did not enter mitosis until 10 hours post thymidine block, (supplementary Fig. 4A) cells were collected 10 −18 hours post release. Thymidine block release in scramble cells resulted in a decrease in percent S phase cells and a corresponding increase in G2/M cells from 10 – 14 hrs, indicating increasing mitotic entry. By 16 and 18 hours, the G2/M cell percent declined, with an increasing G1 percent indicating that cells had begun to slowly exit mitosis and enter G1, all indicative of a regular cell cycle progression (Figure 3C). In comparison, silencing PBK blocked cells at G1 as opposed to S phase observed in controls (Fig3C). Following release, however, the percent of cells in G1 did not decline through 10 to 18 hours showing lack of S phase entry. Furthermore compared to 10 hrs, G2/M or S phase remained unchanged through 12 to 18 hours indicating a large delay in mitotic entry or exit. We also plotted average G2/M and S phase cell percent from 3 independent replicates (Fig. 3 D). Taken together, these data confirmed that partial silencing of PBK, was unable to to block cell cycle progression, but altered the duration of cell cycle phases. PBK silenced cells progressed more slowly through G1 to S and G2/M causing cells to proliferate slowly compared to controls.

Since prolonged mitosis has been shown to induce apoptosis, we analyzed whether stable PBK knockdown induced apoptosis in ACC tumor cells. No significant change in cleaved PARP or caspase 3 was observed between control and PBK silenced cells, suggesting that direct modulation of PBK expression has no effect on cell apoptotic cell death through PARP and caspase-3 pathways (Supplementary Fig. 5).

Pharmacological inhibition of PBK with HITOPK032 inhibits tumorigenic phenotype in ACC cell lines

With the future goal of targeting PBK in patients with ACC, we next examined effects of the available PBK small molecule inhibitor HITOPK032. The PBK inhibitor, HITOPK032, has been shown to target PBK activity (Kim et al. 2012) at doses less than 40uM (Joel et al. 2015) and suppresses *in vitro* kinase activity at doses of 2–5uM (Kim et al. 2012). Using proliferation and clonogenicity assays as outcome measures, we tested the long-term cytostatic effects of HITOPK032 at concentrations ~ 5–25- fold lower than its reported IC50 (Kim et al. 2012).

As shown in Fig. 4A-C, cells were treated with 200nM-1uM of HITOPK032 and rates of ACC cell proliferation by live cell imaging were monitored over 8 days. All three ACC cell lines demonstrated dose dependent responses to the PBK inhibitor with significant inhibition in proliferation by day 8 at doses ranging from 600nM-1uM ($P < 0.01$). The highest dose tested (1uM) proved to be the most effective dose in inhibiting proliferation at time points as early as day 3 in all cell lines.

Colony forming ability of ACC cells was also impaired with HITOPK032 treatment. Cells were plated at low density and monitored for 14 days (Fig. 4D-F), and all were sensitive to HITOPK032 inhibition and exhibited a dose dependent attenuation of colony formation with doses between (50–300) nM ($p < 0.01$). Anchorage independent growth was not measured as the drug failed to consistently penetrate soft agar layers making data interpretation difficult between experiments.

HITOPK032 treatment decreased histone 3 phosphorylation, Akt phosphorylation and induced apoptosis via activation of JNK in ACC cells

Since proliferation assays suggested that at least 1uM of HITOPK032 was required to successfully inhibit proliferation at early time points compared to lower doses with long term exposure, cells were treated with 0–4uM of HITOPK032 for 24 hours to analyze downstream signaling. At these doses, HITOPK032 did not alter PBK gene expression (Fig. 4G) or the cyclin dependent kinase 1 (CDK1) dependent phosphorylation site at Threonine 9 indicating that HITOPK032 does not directly modulate PBK at that specific site (Fig. 4G). HITOPK032 treatment decreased phosphorylation of Akt and histone 3 in all cell lines (Fig. 4G) with no effects on pMEK or its substrate ERK1/2. Multiple experimental replicates revealed that the decrease in Akt activation was most significant at 4uM and ranged from 1.4–1.8-fold across ACC cell lines ($p<0.05$). A dose dependent decrease in pH3 was observed at 2 and 4uM. CU-ACC1 and H295R cells appeared more sensitive to HITOPK032 than CU-ACC2 with both cell lines exhibiting a 3-fold average decrease in histone 3 phosphorylation ($p<0.05$) (Fig. 4G).

To determine if HITOPK032 affected cellular survival, apoptosis in HITOPK032 treated cell lines was measured at 24 and 48 hours assessing cleaved caspase-3 and PARP as markers of cell death (Fig. 5A). Concentrations of HITOPK032 of 1uM and higher elicited a dose dependent apoptotic response at 48hrs in all cell lines ($p < 0.05$). CU-ACC1 cells were more sensitive to HITOPK032 treatment with increased PARP and caspase-3 cleavages at a dose of 1uM as early as 24 hours ($p< 0.01$). The highest dose of HITOPK032 (4uM) induced apoptosis in all cell lines at 24 hours ($p<0.01$).

In nasopharyngeal carcinoma, HITOPK032 has been implicated in stress induction via activation of JNK (Wang et al. 2016). We observed similar activation of JNK/SAPK in CU-ACC1 and H295R cell lines treated with HITOPK032 at doses from 0–4uM. CU-ACC2 cells did not show any significant JNK activation (Fig. 5B). To investigate if pJNK contributed to HITOPK032 mediated apoptosis, we pre-treated CU-ACC1 and H295R cells with SP600125 (10uM), the pJNK inhibitor, overnight. Cells were then incubated with 4uM HITOPK032 in the absence or presence of specific signaling pathway inhibitors for 24 hours before caspase activation was measured (Fig. 5C). Treatment with HITOPK032 induced a 2-fold increase in caspase activation in CU-ACC1 and H295R cells compared to controls (Fig. 5C). Combination treatment with the JNK inhibitor SP600125 (10uM) with HITOPK032 (4uM) resulted in 1.2-fold decrease in caspase activation in CU-ACC1 and a 1.5-fold reduction in H295R cell lines compared to only HITOPK032 (4uM) treated cells, suggesting that induction of apoptosis in ACC cell lines in response to HITOPK032 treatment is in part through JNK activation.

Targeting of PBK inhibits tumor growth in CU-ACC1 PDX model in athymic nude mice

We next pharmacologically targeted PBK in ACC PDX tumor models in athymic nude mice (Kiseljak-Vassiliades et al. 2018a). CU-ACC1 PDX animals were randomized into control and HITOPK032 treatment groups with average tumor size of 198 cm^3 in control group and 139 cm^3 in the treatment group, ($p=0.13$). At the initiation of the study there were 7 trackable tumors in the control and 11 in the treated groups, but three mice in the treatment

group had to be sacrificed early because of skin bruising resulting in 8 HITOPK032 treated tumors at the completion of the study. Mice were dosed at 10mg/kg once daily by oral gavage for 17 days. Figure 6A shows significant decreases in the rate of tumor growth by day 14 and 17 in the HITOPK032 group compared to controls ($p<0.01$) with representative images of tumors harvested at the completion of the study (Fig. 6B). There was wide variability in the rates of tumor growth in the control group; therefore, changes in individual tumor volume through the length of the study are also depicted to show individual tumor response (Fig. 6C). Body weight of the mice was used as an indicator of toxicity and no significant difference between the treated and the control group was observed (Fig. 6D).

Representative tumor tissue from each mouse in the control and treated group was analyzed for pH3, and PARP and caspase-3 cleavage to assess apoptosis. HITOPK032 treated tissues (N= 8) showed a 1.9-fold decrease in pH3 compared to controls (N= 7) as measured by immunohistochemistry (Fig. 6E). Cleaved PARP and caspase-3 was higher in 6 out 7 treated tumors compared to 1 out of 5 tumors in the control group, suggesting that HITOPK032 treatment induced an apoptotic response in ACC PDX tumors (Fig. 6F). There was also an increase in pJNK and a decrease in pAkt expression in the treated tissues compared to controls (Fig. 6F). Taken together, these results confirm that the *in vivo* effects recapitulated the *in vitro* effects of HITOPK032 treatment to inhibit ACC tumorigenesis.

Discussion

ACC is an understudied cancer largely unresponsive to currently available systemic treatments (Armignacco, et al. 2018). In this study, we have identified the mitotic kinase, PBK, as a highly expressed and a putative therapeutic target in ACC. In contrast to normal tissues, PBK is overexpressed in various cancers and is a predictor of adverse clinical outcomes (Chang et al. 2016; Kwon, et al. 2016; Luo, et al. 2014; Ohashi, et al. 2016), but only a handful of studies have examined the mechanistic role of PBK in tumorigenesis.

Here, we have provided supporting evidence for PBK's role in ACC tumorigenesis using cell lines derived from human ACC tumors with different genetic background (Kiseljak-Vassiliades et al. 2018a) and with varied level of PBK expression. Overall our studies demonstrate that ACC cell lines such as H295R and CU-ACC1, which have higher level of PBK expression are reliant on the mitotic kinase to drive their growth phenotype although their background heterogeneity dictates the extent to which PBK dependent downstream effectors modulate various pro proliferative and pro tumorigenic pathways. Phosphorylation p38MAPK and of H3, which have been shown to be direct targets of PBK appeared to be key common effectors of PBK mediated growth (Fig. 4G) in all cell lines. For an indirect target such as Akt, PBK silencing decreased Akt activation in CU-ACC1 and H295R cells but not in CU-ACC2 cell lines. CU-ACC2, which also had the lowest level of PBK expression, also appeared resistant to PBK silencing as observed in the proliferative assays.

In breast cancer, PBK silencing inhibited pH3 and led to dysfunction of cytokinesis promoting apoptosis (Park et al. 2006). We showed that PBK knockdown did not induce apoptosis in ACC cell lines. In the prototype CU-ACC1 cells, PBK knockdown caused a greatly delayed G2/M phase and, the initial G1 accumulation upon thymidine treatment.

This was in contrast to an S phase accumulation observed in the control cells with the double thymidine block. Moreover, the initial G1 accumulation increased through 18 hours post release suggesting that PBK silencing in CU-ACC1 allowed more cells to accumulate at G1 at any given time. This observation was also in agreement with the severe growth restricted phenotype observed upon PBK knockdown in CU-ACC1 cell lines. Hence, rather than triggering apoptosis, PBK silencing restricted the ability of the cell lines, especially CU-ACC1, to proliferate as evidenced by the growth curves shown in Figure 2A. H295R cells, which have a non-functional p53 (Sampaoli, et al. 2012) and activated beta catenin appeared to be resilient to cell cycle alteration with PBK knockdown and also exhibited less alterations in rates proliferation than CU-ACC1.

To examine whether PBK can be effectively targeted via a small molecule inhibitor, we used HITOPK032, a putative PBK inhibitor (Kim et al. 2012). HITOPK032 recapitulated shPBK specific effects by inhibiting pH3 and pAkt in H295R, CU-ACC1, and CU-ACC2 cell lines, but in addition, induced apoptosis via activation of JNK. These data suggest that HITOPK032 acts via PBK independent stress pathways. Prior studies have defined a role of PBK in the DNA damage response (Ayllon and O'Connor 2007). Although further studies are required to determine causes behind JNK activation, we hypothesize that a component of the HITOPK032 mediated effects may be dependent on a DNA damage response in ACC tumors. Another possibility is that similar to nasopharyngeal carcinoma, HITOPK032 treatment of ACC induced reactive oxygen species and ER stress (Wang et al. 2016).

Examining the efficacy of therapeutic targeting in *in vivo* models which closely recapitulate human tumors (Tentler, et al. 2012) has been a long unmet need in the field of ACC. We showed that HITOPK032 effectively inhibited tumor growth using the first PDX model in the field of adult ACC. PDXs have been shown to have minimal drift (Tentler et al. 2012) from the matching tumor in early passages and represent human tumorigenesis with respect to tumor architecture, gene signature, stroma and mutational signature. Treatment responses in PDX are more reflective of the clinical drug's effectiveness than xenograft in vivo studies (Tentler et al. 2012).We have also validated downstream effectors of HITOPK032 in the harvested PDX tumor tissues demonstrating that the *in vivo* responses closely recapitulated effects of *in vitro* experiments, which is encouraging for future target development.

In summary, we have shown that targeting PBK, both genomically and pharmacologically, inhibits tumorigenic growth in preclinical models of ACC. Our data suggest that targeting with HITOPK032 may be more effective than PBK silencing alone since HITOPK032 induces additional PBK-independent cell death, the mechanism of which requires additional investigation. Moreover, our data provides early indications that HITOPK032 is able to trigger stress response pathways. Mitotane, an adrenolytic drug used to treat patients with ACC has been shown to cause ER stress (Sbiera, et al. 2015). Studies with H295R cells have shown that Mitotane at low concentrations can be paired with other chemotherapeutic drugs to synergistically antagonize tumor growth (De Martino, et al. 2016). Future investigations will test in our new preclinical models the hypothesis that disruption of specific components of the cell the cycle such as PBK in conjunction with Mitotane, a known ER stress inducer, will enhance the anti-tumorigenic responses in ACC and provide new treatment strategies for our patients with ACC.

Supplementary Material

Refer to Web version on PubMed Central for supplementary material.

Acknowledgements

We thank the University of Colorado (UCD) Laboratory Animal Resources, Protein production/MoAb/Tissue culture core, Flow cytometry shared resource facility (FCSR), Genomics and Genomics and Miroarray core for providing space and services for acquisition of data. We thank Dr. Lauren Fishbein (Endocrinology, UCD) for reviewing the manuscript.

Funding : This work was supported by NIH K12CA086913–12 (to K.K.V), NIH K08CA222620 (to K.K.V.), Cancer League of Colorado Award (to K.K.V. and S.L.), Doris Duke CU-FSRC (to K.K.V.), Veterans Affairs Merit Review Award 001 (to M.E.W.), University of Colorado Cancer Center Support Grant P30-CA046934. The funding bodies had no role in the design of the study and collection, analysis, and interpretation of data or in writing the manuscript.

References

Abe Y, Takeuchi T, Kagawa-Miki L, Ueda N, Shigemoto K, Yasukawa M & Kito K 2007 A mitotic kinase TOPK enhances Cdk1/cyclin B1-dependent phosphorylation of PRC1 and promotes cytokinesis. J Mol Biol 370 231–245. [PubMed: 17512944]

Armignacco R, Cantini G, Canu L, Poli G, Ercolino T, Mannelli M & Luconi M 2018 Adrenocortical carcinoma: the dawn of a new era of genomic and molecular biology analysis. J Endocrinol Invest 41 499–507. [PubMed: 29080966]

Assie G, Letouze E, Fassnacht M, Jouinot A, Luscap W, Barreau O, Omeiri H, Rodriguez S, Perlemoine K, Rene-Corail F, et al. 2014 Integrated genomic characterization of adrenocortical carcinoma. Nat Genet 46 607–612. [PubMed: 24747642]

Ayllon V & O'Connor R 2007 PBK/TOPK promotes tumour cell proliferation through p38 MAPK activity and regulation of the DNA damage response. Oncogene 26 3451–3461. [PubMed: 17160018]

Barlaskar FM, Spalding AC, Heaton JH, Kuick R, Kim AC, Thomas DG, Giordano TJ, Ben-Josef E & Hammer GD 2009 Preclinical targeting of the type I insulin-like growth factor receptor in adrenocortical carcinoma. The Journal of clinical endocrinology and metabolism 94 204–212. [PubMed: 18854392]

Berruti A, Grisanti S, Pulzer A, Claps M, Daffara F, Loli P, Mannelli M, Boscaro M, Arvat E, Tiberio G, et al. 2017 Long-Term Outcomes of Adjuvant Mitotane Therapy in Patients With Radically Resected Adrenocortical Carcinoma. J Clin Endocrinol Metab 102 1358–1365. [PubMed: 28324035]

Beuschlein F, Jakoby J, Mentz S, Zambetti G, Jung S, Reincke M, Suss R & Hantel C 2016 IGF1-R inhibition and liposomal doxorubicin: Progress in preclinical evaluation for the treatment of adrenocortical carcinoma. Mol Cell Endocrinol 428 82–88. [PubMed: 26994514]

Boulle N, Baudin E, Gicquel C, Logie A, Bertherat J, Penfornis A, Bertagna X, Luton JP, Schlumberger M & Le Bouc Y 2001 Evaluation of plasma insulin-like growth factor binding protein-2 as a marker for adrenocortical tumors. Eur J Endocrinol 144 29–36. [PubMed: 11174834]

Brown-Clay JD, Shenoy DN, Timofeeva O, Kallakury BV, Nandi AK & Banerjee PP 2015 PBK/TOPK enhances aggressive phenotype in prostate cancer via beta-catenin-TCF/LEF-mediated matrix metalloproteinases production and invasion. Oncotarget 6 15594–15609. [PubMed: 25909225]

Cerami E, Gao J, Dogrusoz U, Gross BE, Sumer SO, Aksoy BA, Jacobsen A, Byrne CJ, Heuer ML, Larsson E, et al. 2012 The cBio cancer genomics portal: an open platform for exploring multidimensional cancer genomics data. Cancer Discov 2 401–404. [PubMed: 22588877]

Chang CF, Chen SL, Sung WW, Hsieh MJ, Hsu HT, Chen LH, Chen MK, Ko JL, Chen CJ & Chou MC 2016 PBK/TOPK Expression Predicts Prognosis in Oral Cancer. Int J Mol Sci 17.

Chau NG, Hotte SJ, Chen EX, Chin SF, Turner S, Wang L & Siu LL 2012 A phase II study of sunitinib in recurrent and/or metastatic adenoid cystic carcinoma (ACC) of the salivary glands: current progress and challenges in evaluating molecularly targeted agents in ACC. Ann Oncol 23 1562–1570. [PubMed: 22080184]

De Martino MC, van Koetsveld PM, Feelders RA, Lamberts SW, de Herder WW, Colao A, Pivonello R & Hofland LJ 2016 Effects of combination treatment with sirolimus and mitotane on growth of human adrenocortical carcinoma cells. Endocrine 52 664–667. [PubMed: 26645813]

Dou X, Wei J, Sun A, Shao G, Childress C, Yang W & Lin Q 2015 PBK/TOPK mediates geranylgeranylation signaling for breast cancer cell proliferation. Cancer Cell Int 15 27. [PubMed: 25745361]

Else T, Kim AC, Sabolch A, Raymond VM, Kandathil A, Caoili EM, Jolly S, Miller BS, Giordano TJ & Hammer GD 2014 Adrenocortical carcinoma. Endocr Rev 35 282–326. [PubMed: 24423978]

Fassnacht M, Berruti A, Baudin E, Demeure MJ, Gilbert J, Haak H, Kroiss M, Quinn DI, Hesseltine E, Ronchi CL, et al. 2015 Linsitinib (OSI-906) versus placebo for patients with locally advanced or metastatic adrenocortical carcinoma: a double-blind, randomised, phase 3 study. Lancet Oncol 16 426–435. [PubMed: 25795408]

Gao J, Aksoy BA, Dogrusoz U, Dresdner G, Gross B, Sumer SO, Sun Y, Jacobsen A, Sinha R, Larsson E, et al. 2013 Integrative analysis of complex cancer genomics and clinical profiles using the cBioPortal. Sci Signal 6 pl1. [PubMed: 23550210]

Hahner S & Fassnacht M 2005 Mitotane for adrenocortical carcinoma treatment. Curr Opin Investig Drugs 6 386–394.

He F, Yan Q, Fan L, Liu Y, Cui J, Wang J, Wang L, Wang Y, Wang Z, Guo Y, et al. 2010 PBK/TOPK in the differential diagnosis of cholangiocarcinoma from hepatocellular carcinoma and its involvement in prognosis of human cholangiocarcinoma. Hum Pathol 41 415–424. [PubMed: 19954816]

Hu F, Gartenhaus RB, Eichberg D, Liu Z, Fang HB & Rapoport AP 2010 PBK/TOPK interacts with the DBD domain of tumor suppressor p53 and modulates expression of transcriptional targets including p21. Oncogene 29 5464–5474. [PubMed: 20622899]

Joel M, Mughal AA, Grieg Z, Murrell W, Palmero S, Mikkelsen B, Fjerdingstad HB, Sandberg CJ, Behnan J, Glover JC, et al. 2015 Targeting PBK/TOPK decreases growth and survival of glioma initiating cells in vitro and attenuates tumor growth in vivo. Mol Cancer 14 121. [PubMed: 26081429]

Kar A & Gutierrez-Hartmann A 2017 ESE-1/ELF3 mRNA expression associates with poor survival outcomes in HER2(+) breast cancer patients and is critical for tumorigenesis in HER2(+) breast cancer cells. Oncotarget 8 69622–69640. [PubMed: 29050229]

Kato T, Inoue H, Imoto S, Tamada Y, Miyamoto T, Matsuo Y, Nakamura Y & Park JH 2016 Oncogenic roles of TOPK and MELK, and effective growth suppression by small molecular inhibitors in kidney cancer cells. Oncotarget 7 17652–17664. [PubMed: 26933922]

Kim DJ, Li Y, Reddy K, Lee MH, Kim MO, Cho YY, Lee SY, Kim JE, Bode AM & Dong Z 2012 Novel TOPK inhibitor HI-TOPK-032 effectively suppresses colon cancer growth. Cancer Res 72 3060–3068. [PubMed: 22523035]

Kiseljak-Vassiliades K, Zhang Y, Bagby SM, Kar A, Pozdeyev N, Xu M, Gowan K, Sharma V, Raeburn CD, Albuja-Cruz M, et al. 2018a Development of new preclinical models to advance adrenocortical carcinoma research. Endocr Relat Cancer 25 437–451. [PubMed: 29371329]

Kiseljak-Vassiliades K, Zhang Y, Kar A, Razzaghi R, Xu M, Gowan K, Raeburn CD, Albuja-Cruz M, Jones KL, Somerset H, et al. 2018b Elucidating the Role of the Maternal Embryonic Leucine Zipper Kinase (MELK) in Adrenocortical Carcinoma. Endocrinology.

Kwon CH, Park HJ, Choi YR, Kim A, Kim HW, Choi JH, Hwang CS, Lee SJ, Choi CI, Jeon TY, et al. 2016 PSMB8 and PBK as potential gastric cancer subtype-specific biomarkers associated with prognosis. Oncotarget 7 21454–21468. [PubMed: 26894977]

Lei B, Liu S, Qi W, Zhao Y, Li Y, Lin N, Xu X, Zhi C, Mei J, Yan Z, et al. 2013 PBK/TOPK expression in non-small-cell lung cancer: its correlation and prognostic significance with Ki67 and p53 expression. Histopathology 63 696–703. [PubMed: 24025073]

Libe R 2015 Adrenocortical carcinoma (ACC): diagnosis, prognosis, and treatment. Front Cell Dev Biol 3 45. [PubMed: 26191527]

Luo Q, Lei B, Liu S, Chen Y, Sheng W, Lin P, Li W, Zhu H & Shen H 2014 Expression of PBK/TOPK in cervical cancer and cervical intraepithelial neoplasia. Int J Clin Exp Pathol 7 8059–8064. [PubMed: 25550851]

Matsumoto S, Abe Y, Fujibuchi T, Takeuchi T, Kito K, Ueda N, Shigemoto K & Gyo K 2004 Characterization of a MAPKK-like protein kinase TOPK. Biochem Biophys Res Commun 325 997–1004. [PubMed: 15541388]

Matsuo Y, Park JH, Miyamoto T, Yamamoto S, Hisada S, Alachkar H & Nakamura Y 2014 TOPK inhibitor induces complete tumor regression in xenograft models of human cancer through inhibition of cytokinesis. Sci Transl Med 6 259ra145.

Mohan DR, Lerario AM & Hammer GD 2018 Therapeutic Targets for Adrenocortical Carcinoma in the Genomics Era. J Endocr Soc 2 1259–1274. [PubMed: 30402590]

Nandi AK, Ford T, Fleksher D, Neuman B & Rapoport AP 2007 Attenuation of DNA damage checkpoint by PBK, a novel mitotic kinase, involves protein-protein interaction with tumor suppressor p53. Biochem Biophys Res Commun 358 181–188. [PubMed: 17482142]

Ohashi T, Komatsu S, Ichikawa D, Miyamae M, Okajima W, Imamura T, Kiuchi J, Kosuga T, Konishi H, Shiozaki A, et al. 2017 Overexpression of PBK/TOPK relates to tumour malignant potential and poor outcome of gastric carcinoma. Br J Cancer 116 218–226. [PubMed: 27898655]

Ohashi T, Komatsu S, Ichikawa D, Miyamae M, Okajima W, Imamura T, Kiuchi J, Nishibeppu K, Kosuga T, Konishi H, et al. 2016 Overexpression of PBK/TOPK Contributes to Tumor Development and Poor Outcome of Esophageal Squamous Cell Carcinoma. Anticancer Res 36 6457–6466. [PubMed: 27919968]

Park JH, Lin ML, Nishidate T, Nakamura Y & Katagiri T 2006 PDZ-binding kinase/T-LAK cell-originated protein kinase, a putative cancer/testis antigen with an oncogenic activity in breast cancer. Cancer Res 66 9186–9195. [PubMed: 16982762]

Park JH, Nishidate T, Nakamura Y & Katagiri T 2010 Critical roles of T-LAK cell-originated protein kinase in cytokinesis. Cancer Sci 101 403–411. [PubMed: 19900192]

Quinkler M, Hahner S, Wortmann S, Johanssen S, Adam P, Ritter C, Strasburger C, Allolio B & Fassnacht M 2008 Treatment of advanced adrenocortical carcinoma with erlotinib plus gemcitabine. J Clin Endocrinol Metab 93 2057–2062. [PubMed: 18334586]

Rizkallah R, Batsomboon P, Dudley GB & Hurt MM 2015 Identification of the oncogenic kinase TOPK/PBK as a master mitotic regulator of C2H2 zinc finger proteins. Oncotarget 6 1446–1461. [PubMed: 25575812]

Sampaoli C, Cerquetti L, Gawhary RE, Bucci B, Amendola D, Marchese R, Misiti S, Novelli G, Toscano V & Stigliano A 2012 p53 Stabilization induces cell growth inhibition and affects IGF2 pathway in response to radiotherapy in adrenocortical cancer cells. PLoS One 7 e45129. [PubMed: 23028800]

Sbiera S, Leich E, Liebisch G, Sbiera I, Schirbel A, Wiemer L, Matysik S, Eckhardt C, Gardill F, Gehl A, et al. 2015 Mitotane Inhibits Sterol-O-Acyl Transferase 1 Triggering Lipid-Mediated Endoplasmic Reticulum Stress and Apoptosis in Adrenocortical Carcinoma Cells. Endocrinology 156 3895–3908. [PubMed: 26305886]

Shinde SR, Gangula NR, Kavela S, Pandey V & Maddika S 2013 TOPK and PTEN participate in CHFR mediated mitotic checkpoint. Cell Signal 25 2511–2517. [PubMed: 24012691]

Stauffer S, Zeng Y, Zhou J, Chen X, Chen Y & Dong J 2017 CDK1-mediated mitotic phosphorylation of PBK is involved in cytokinesis and inhibits its oncogenic activity. Cell Signal 39 74–83. [PubMed: 28780319]

Tentler JJ, Tan AC, Weekes CD, Jimeno A, Leong S, Pitts TM, Arcaroli JJ, Messersmith WA & Eckhardt SG 2012 Patient-derived tumour xenografts as models for oncology drug development. Nat Rev Clin Oncol 9 338–350. [PubMed: 22508028]

Terzolo M, Daffara F, Ardito A, Zaggia B, Basile V, Ferrari L & Berruti A 2014 Management of adrenal cancer: a 2013 update. J Endocrinol Invest 37 207–217. [PubMed: 24458831]

Wang MY, Lin ZR, Cao Y, Zheng LS, Peng LX, Sun R, Meng DF, Xie P, Yang JP, Cao L, et al. 2016 PDZ binding kinase (PBK) is a theranostic target for nasopharyngeal carcinoma: driving tumor

growth via ROS signaling and correlating with patient survival. Oncotarget 7 26604–26616. [PubMed: 27049917]

Wang T & Rainey WE 2012 Human adrenocortical carcinoma cell lines. Mol Cell Endocrinol 351 58–65. [PubMed: 21924324]

Zheng S, Cherniack AD, Dewal N, Moffitt RA, Danilova L, Murray BA, Lerario AM, Else T, Knijnenburg TA, Ciriello G, et al. 2016 Comprehensive Pan-Genomic Characterization of Adrenocortical Carcinoma. Cancer Cell 29 723–736. [PubMed: 27165744]

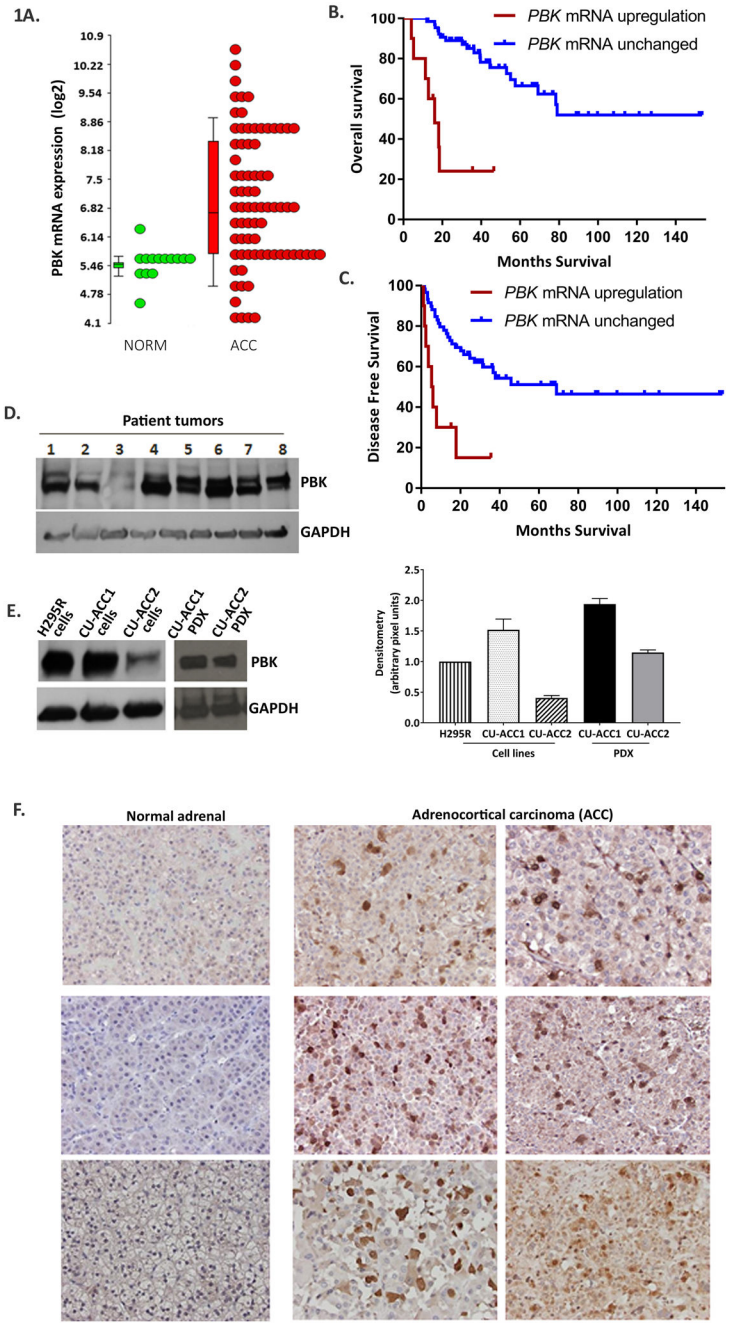

Figure 1.

PBK is overexpressed in ACC tumors and dictates survival outcomes. **A.** *PBK* mRNA expression in ACC (n=77) is 12 fold higher than normal adrenal tissues (n=14) and 7 fold higher than adenomas (n=22) in microarray gene expression studies. **B,C.** Kaplan Meier analysis of survival using Graph Pad Prism with normalized RNA seq data from the TCGA cohort of ACC (n=75) available in cbioportal. RNA expression was normalized using RSEM.10% of the population in TCGA cohort had a Z s core >2 and was designated to have PBK mRNA upregulation. High *PBK* expression associated with poor overall survival (OS) and poorer disease free survival (DFS) (** p< 0.01). **D, E.** PBK protein expression in ACC

tumor tissues and ACC cell lines and PDXs. Quantification of E is shown on the right F. IHC with anti-PBK in normal adrenal show no nuclear staining but strong nuclear and diffused cytoplasmic staining in ACC.

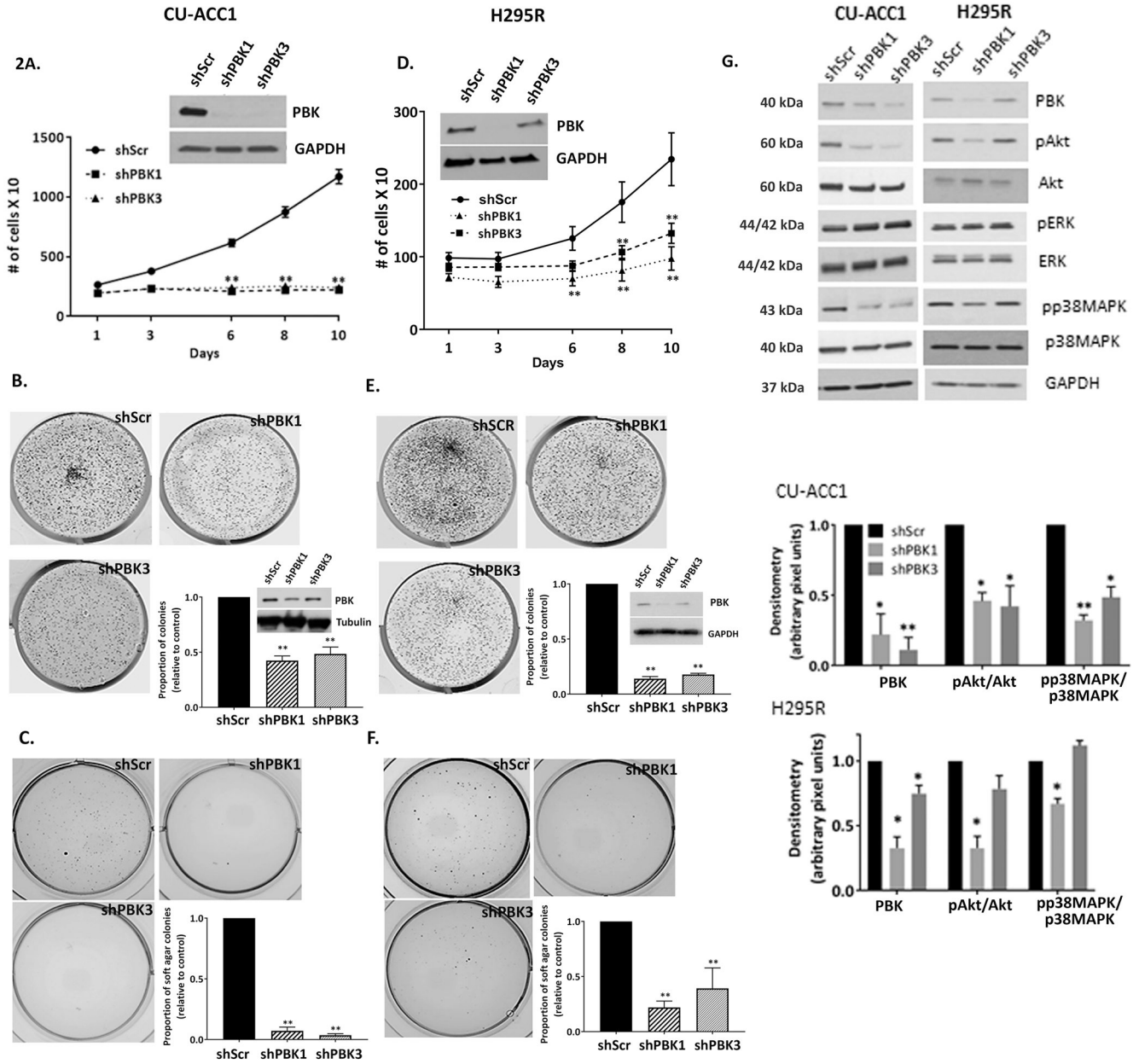

Figure 2.

PBK knockdown inhibits cell proliferation, clonogenicity, and soft agar colony formation in ACC. **A, D.** PBK silencing attenuates proliferation in CU-ACC1 and H295R cell lines. **B,E.** PBK knockdown causes on average a ~2 fold decrease in colony formation in CU-ACC1 and on average a ~ 6 fold decrease in H295R. **C, F.** Knocking down PBK significantly inhibits anchorage independent growth by ~20 fold in CU-ACC1 and by (4-6) fold in H295R cell lines. **G.** Immunoblot showing decrease in p-Akt, p-p38MAPK, and no change in pERKf with PBK knockdown in CU-ACC1 and H295R cell lines. Data presented has been derived from at least 3 biological replicates. Data represented as mean +/− SEM (* p <0.05, **p<0.01). Quantification of immunoblots have been done using normalized densitometric values derived at least 3 biological repeats.

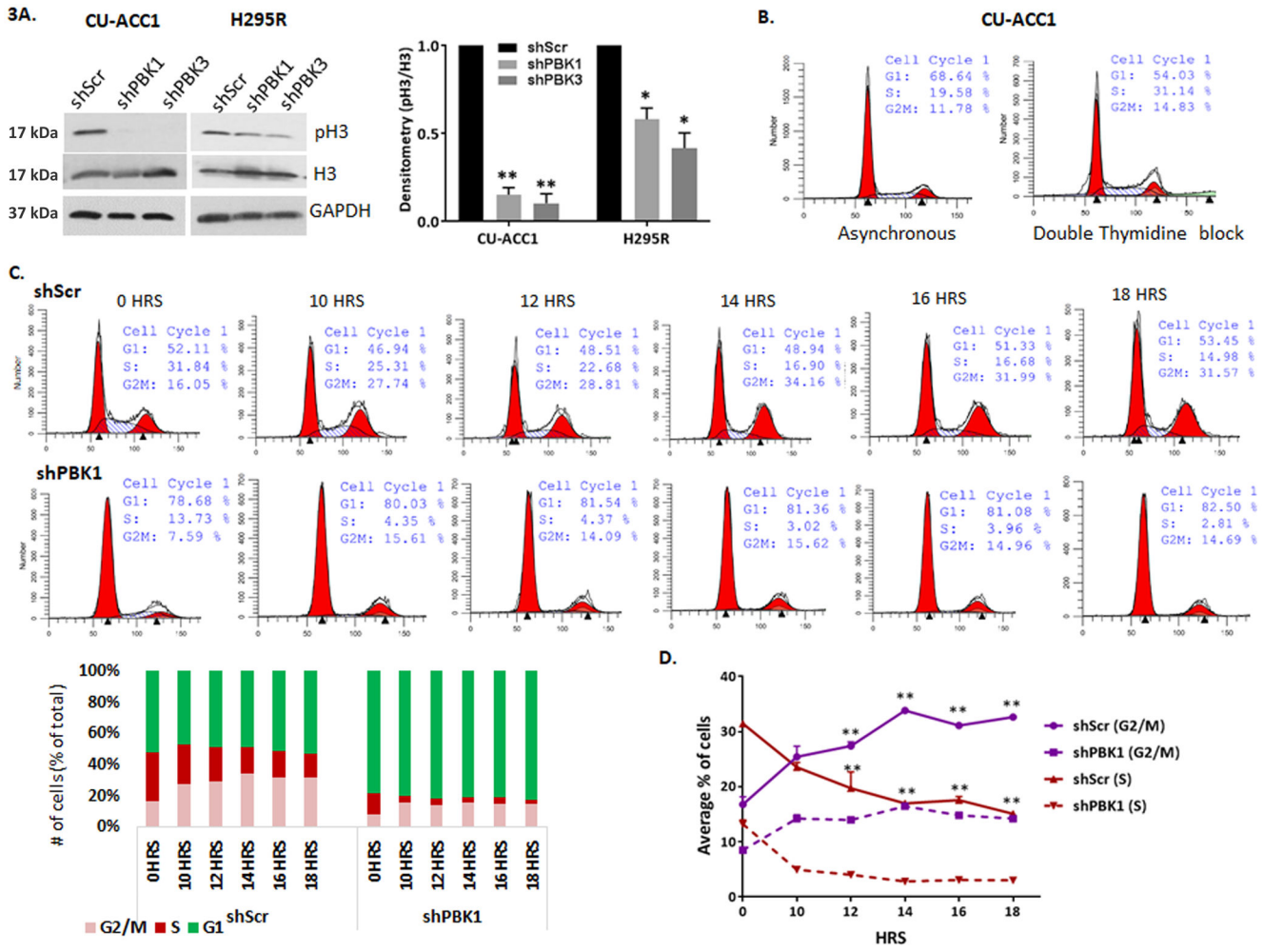

Figure 3.

PBK silencing inhibits H3 phosphorylation and alters cell cycle progression. **A.** PBK knockdown decreased pH3 in CU-ACC1 and H295R cell lines. Knockdown causes on average a 5 fold decrease (** $p<0.01$) in CU-ACC1 and on average 2 fold decrease (*$p < 0.05$) in H295R as assessed by densitometry. **B.** Flow cytometry analysis of asynchronous and double thymidine blocked CU-ACC1 control shscr cells at 0 hours post release showing a 1.6 fold increase in S phase cells in controls. **C.** Cell cycle analysis post thymidine block through 0 to 18 hours, original flow plots and a bar graph visualization of % cell progression through different time points. **D.** Average percent of cells in G2/M and S phase through 0 to 18 hours post release from double thymidine block collected from three experimental replicates. Significant changes in G2/M and S phase cell % in controls through 12 to 18 hours have been denoted by ** $p <0.01$. Data has been derived from three experimental replicates and is represented as mean +/− SEM.

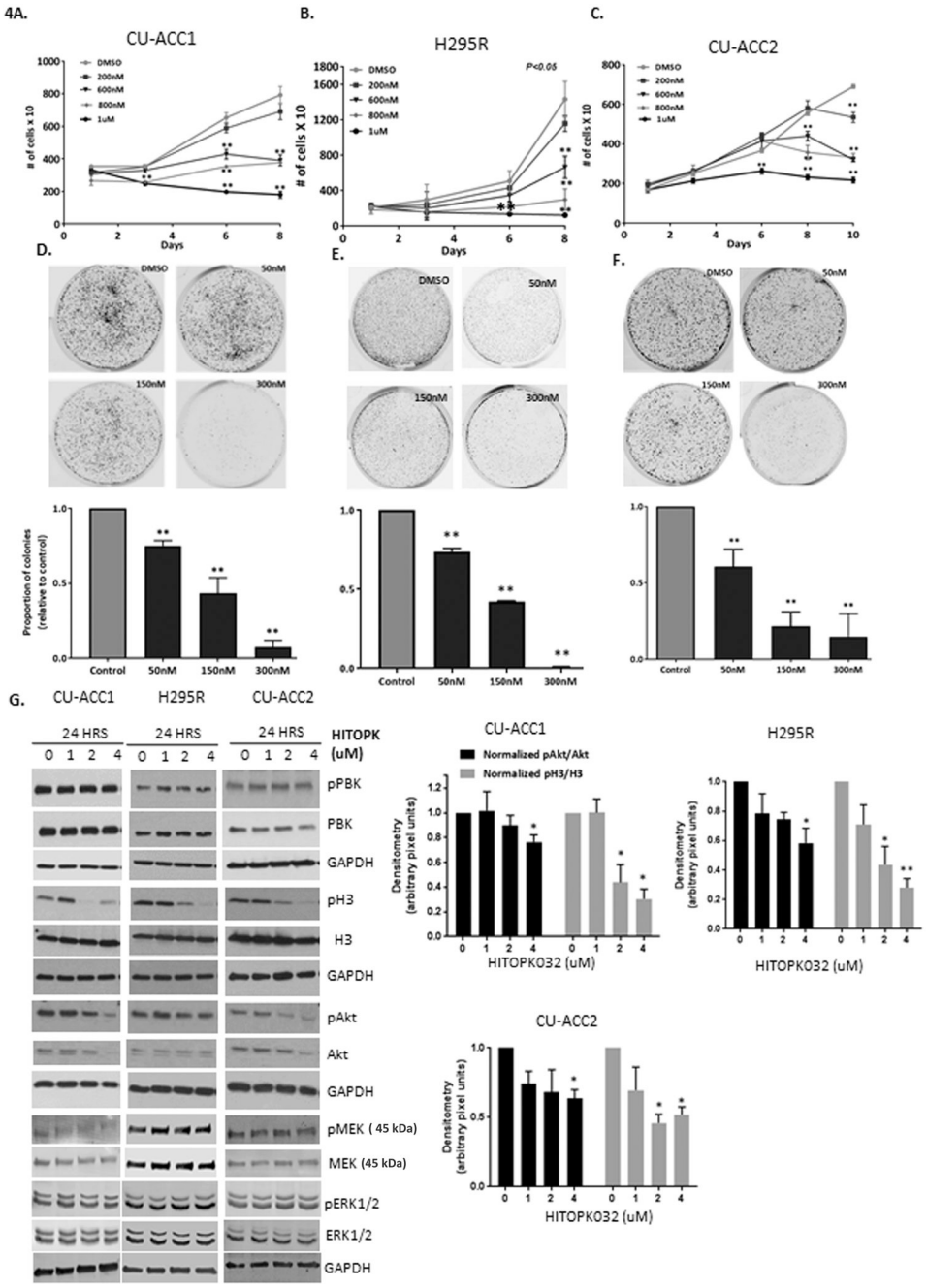

Figure 4.

HITOPK032 treatment inhibits tumorigenic properties and recapitulates effects of PBK silencing in ACC. **A-C.** Cell lines show a dose dependent response to HITOPK032 treatment at 600–1uM range (**P<0.01) by day 8. Graphs shown are representative experiments of 3 biological repeats; data presented as mean +/−SEM.**D-F.** Dose dependent decrease in colony formation to doses of 50 to 300nM of HITOPK032. **G.** HITOPK032 decreases Akt and H3 phosphorylation as shown via immunobloting. P values (**p<0.01, *p<0.05) have been calculated using normalized densitometric values derived from immunoblots of at least 3

biological repeats. All normalization has been done to the DMSO control. Data represented as mean +/− SEM.

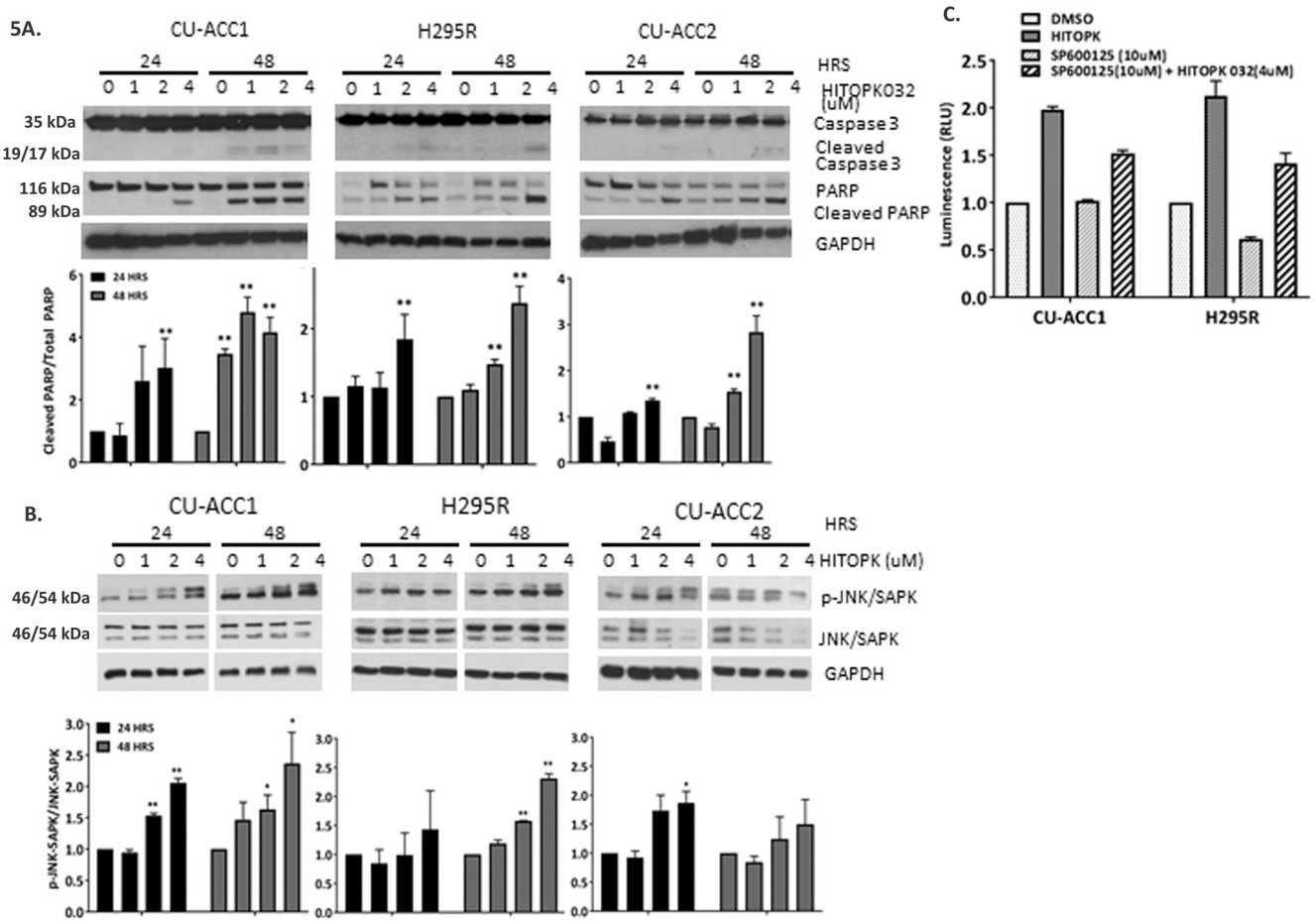

Figure 5.

Apoptosis induced by HITOPK032 is in part mediated by JNK activation. **A**. HITOPK032 at 1uM or higher induces apoptosis in a dose dependent manner by 48 hours in all cell lines. **B**. HITOPK treatment induces JNK phosphorylation in CU-ACC1and H295R cell lines. **C**. Treating CU-ACC1 and H295R cell lines with 10uM of the JNK inhibitor in presence of 4uM HITOPK032 partially inhibits caspase 3/7 activity measured by the caspase 3/7 glo assay. P values (**p<0.01, * p<0.05)) have been calculated from normalized RLU of at least three biological repeats. Quantification of immunoblots have been derived from normalized densitometric values from three independent replicates. All normalization has been done to the DMSO control. Data represented as mean +/−SEM.

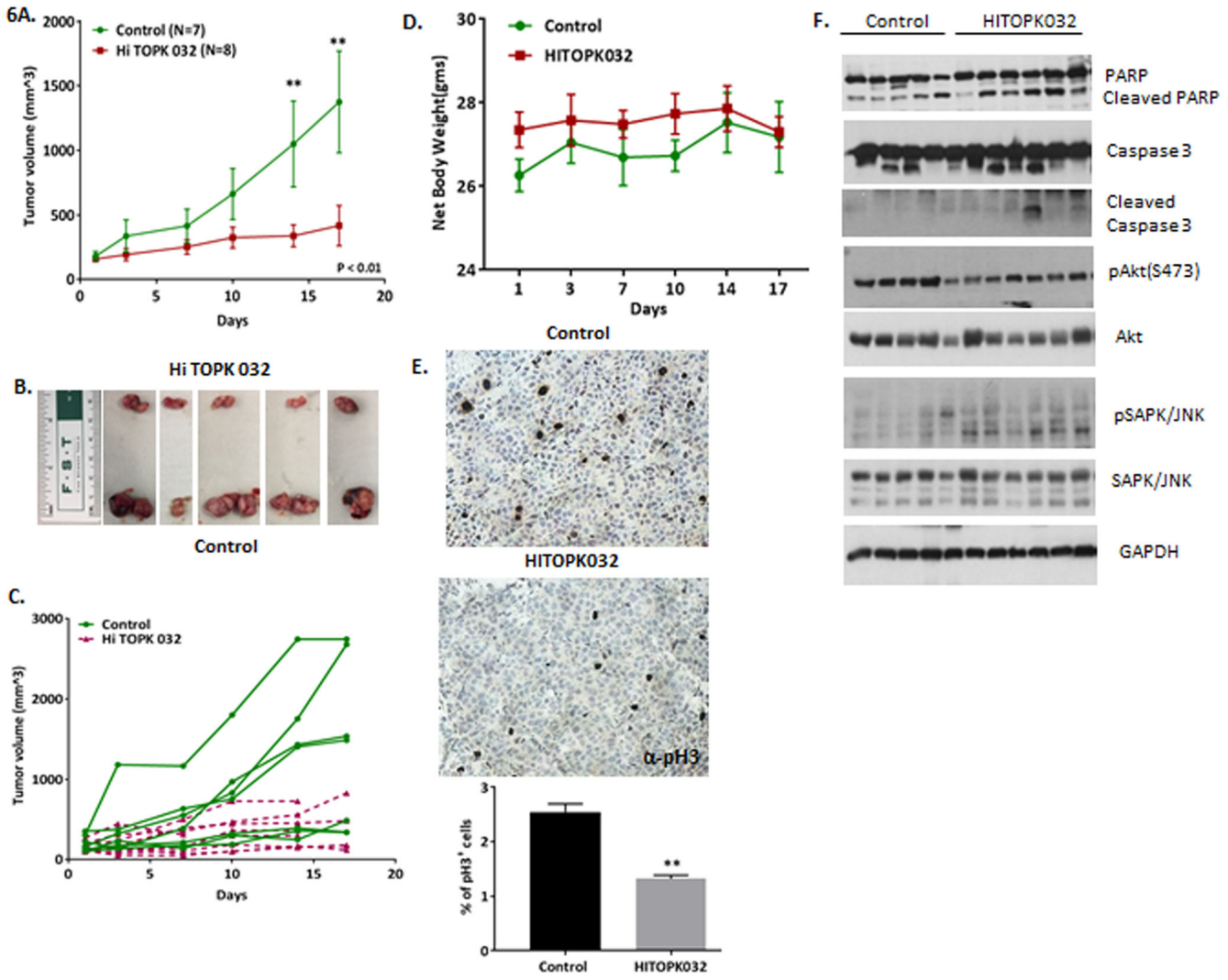

Figure 6.

HITOPK032 inhibits tumorigenic growth in ACC. **A**. HITOPK032 treatment in athymic nude mice bearing passage 14 CU-ACC1 PDXs shows significant decrease in tumor rate by day 14 and day 17 (**p<0.01). **B**. A representative image of tumors harvested at the end of the study. Treated group has smaller tumor size compared to control. **C**. Graph showing growth rates of individual tumors following HITOPK032 treatment. **D**. Average net weight of mice in treated and the control group shows no significant change in body weight. **E**. IHC analysis of pH3 in tissue sections of control and treated tumors. There is 1.9 fold decrease in histone 3 phosphorylation in treated group relative to control (**p<0.01). **F**. Immunoblot of representative tumor lysates from 5 control and 6 treated tumors collected from individual mice showing difference in cleaved PARP, cleaved caspase 3, pAkt and pJNK expression between control and treated group (*p<0.05, **p<0.01)